JOINT EUROPEAN TORUS

JET–P(91)49

I.H. Coffey, F.P. Keenan, C. McAdam, R. Bamsley, W.J. Dickson,
K.D. Lawson, N.J. Peacock and JET Team

Electron Temperature and Density Sensitive X-Ray Enission Line Ratios for CI XVI

Electron Temperature and Density Sensitive X-Ray Enission Line Ratios for CI XVI

I.H. Coffey[1], F.P. Keenan[1], C. McAdam[1], R. Bamsley, W.J. Dickson, K.D. Lawson[2], N.J. Peacock[2] and JET Team*

JET-Joint Undertaking, Culham Science Centre, OX14 3DB, Abingdon, UK

[1]Department of Pure and Applied Physics, Queen's University, Belfast, Northern Ireland.
[2]Culham Laboratory, Abingdon, Oxon, OX14 3DB
** See Appendix 1*

Preprint of Paper to be submitted for publication in
Physica Scripta

ABSTRACT.

Recently calculated electron impact excitation rates for transitions in helium-like Cl XVI are used to derive the electron temperature sensitive emission line ratio G = ((x + y + z)/w) and the electron density sensitive ratio R = (z/(x + y)) where w, x, y and z are the resonance $ls_2\ ^1S_0$ - ls2p $^1P_1$, intercombination $ls^2\ 1S_0$ - ls2p $^3P_{2,1}$ and forbidden $ls^2\ 1S_0$ - ls2s $^3S_1$ transitions, respectively. These calculations, which differ from those of previous authors, are compared with experimental R and G ratios obtained from X-ray spectra from the JET (Joint European Torus) plasma, for which the electron temperature and density have been measured by independent methods. The R ratio is approximately in its low density limit (R_0) for this device and is therefore not electron density sensitive. However it does function as an electron temperature diagnostic as does the G ratio. A comparison is also made with the previously reported results from the Alcator-C tokamak, where the experimental results lie in the electron density sensitive region. The results show good agreement between theory and observation, with discrepancies of typically 7% in R and 10% in G for JET, implying that the theoretical results may be applied to the analysis of remote plasma sources in order to derive values for T_e and N_e where no independent estimates for these parameters exist. A departure from coronal equilibrium due to diffusion effects is taken into account for the JET plasma conditions, and the resulting non-coronal ionisation balance is found to produce changes to the theoretical ratios in regions removed from the centre of the JET plasma.

1. Introduction

Emission lines due to transitions in He-like ions in the soft X-ray spectrum are readily observed in high temperature laboratory plasmas [1,2] as well as the solar corona [3-5] . The principal lines resulting from transitions between the $1s^2\ ^1S_0$ ground state and $1s2l$ levels (see fig.1) are the resonance line w, $1s^2\ ^1S_0$ - $1s2p\ ^1P_1$, x and y the intercombination lines $1s^2\ ^1S_0$ - $1s2p\ ^3P_{2,1}$, and z the forbidden transition $1s^2\ ^1S_0$ - $1s2s\ ^3S_1$. From these the electron density and temperature of the emitting region may be obtained from the line ratios $R=(z/(x+y))$ and $G=((x+y+z)/w)$ [6-7]. Of the remaining two states, the only radiative decay of the 1s2s $^1S_0$ state is through a two photon emission, whereas the 1s2p $^3P_0$ decays radiatively into the 1s2s $^3S_1$ state with the emission of a low energy photon or to the ground state if the nuclear spin $I \neq 0$[8].

In determining theoretical ratios accurate atomic physics data must be employed, especially for electron impact excitation rates from the ground state to the $1s2l$ levels. These calculations have been carried out by several authors [9] including those of Pradhan [10] for Ca XIX and FeXXV using the distorted wave approximation [11] , and those derived using the R-matrix code [12] by Tayal and Kingston [13-15], Kingston and Tayal [16,17] and Tayal [18,19] for C V, O VII and Mg XI.

Keenan et al [20] have used the results of the above authors to interpolate electron excitation rates for transitions between the ground state and $n=2$ and 3 levels for He-like ions between F VII and Mn XXIV. In this paper the R and G emission line ratios for Cl XVI are derived using these data for a plasma in coronal equilibrium. A comparison is made with observed ratios from the JET tokamak for which the R ratio is in its low density limit (R_o) [21,22], and is not electron density sensitive, but does show a degree of electron temperature dependence. The results are also compared with the theoretical and experimental results of Källne et al [23] for which the experimental data lies above the low density limit. A departure from coronal equilibrium is taken into account for the JET plasma conditions, and the resulting non-coronal ionisation balance is found to produce changes to the theoretical ratios in regions removed from the centre of the JET plasma.

2. Atomic data

The model ion for Cl XVI consisted of the 23 lowest $1snl$ states with $n<6$ and $l<3$, making a total of 37 levels when fine structure splitting in the triplet terms was taken into account. Energies of all these levels were taken from Kelly [24] .

Electron impact excitation rates from the $1s^2\ ^1S_0$ ground state to the $n=2$ and 3 levels were obtained from Keenan et al [20] , while for those among the $n=2$ levels the rates were interpolated from Zhang and Sampson [25] data. Rates for transitions to or between higher $1snl$ states were obtained using the n^{-3} scaling law of Gabriel and Heddle [26] , in conjunction with the above.

Einstein A-coefficients were obtained from Lin [27] for transitions from the $n=2$ levels, except for $1s^2\ ^1S_0$ - $1s2p\ ^3P_0$ which is taken from Mohr [8] . Radiative rates from higher states were taken from Laughlin [28] and Kahn and Khandelwal [29] , or extrapolated from the calculations of Cohen and McEachran [30] , Jacobs[31] and Lin et al [32] .

The effects of dielectronic and radiative recombination (Blumenthal et al [7]) of H-like Cl on the Cl XVI level populations are important considerations. These processes are included in the present calculations by employing the rate coefficients of Mewe and Schriver [33] and the coronal ionisation balance ratios of Summers et al [34]. Innershell ionisation of Li-like Cl was found to have minimal effect on the calculated ratios for the density and temperature regions considered in this paper, and has therefore been excluded from the calculations [35]

Proton impact excitation [36] rates have not been included in the model. These can be important for transitions with small excitation energies and have been shown to have significant effects on line ratio calculations carried out for F-like ions using the calculations of Keenan and Reid [37,38] , but test calculations for other He-like ions [39] have shown negligible effects on the level populations in the density regime of the current experiment.

3. Experimental Data

The experimental results were obtained from the JET [40] tokamak, where chlorine appears as an intrinsic impurity in the deuterium plasma. The JET device has major and minor radii of 2.96m and 1.25m respectively, a maximum toroidal field of 3.45T and maximum toroidal current of 7MA. Typical central electron densities and temperatures for the discharges considered are $N_e \simeq 2.5 \times 10^{13}$ cm^{-3} and $T_e \simeq 3 \times 10^7$K respectively.

The spectra were obtained with a double crystal x-ray monochromator [41], which was situated outside the biological shield of the torus hall for maximum shielding from neutrons and hard x-rays. It was used in repetitive scan mode, covering the wavelength region from 4.4Å to 4.5Å, and was calibrated for absolute wavelength and intensity measurements with a resolving power ($\lambda/\delta\lambda$) of $\simeq$4500. The detector was a multiwire proportional counter which could operate at 10MHz.

This instrument provided central chord integrated signals. To determine the radial position of maximum emissivity for Cl XVI a transport code [42] was utilised, which calculated radial profiles of intensity, density and radiated power for all the ionisation stages of a particular impurity element at a given time during a discharge. Electron temperature and density measurements at the radial positions thus determined were found from radial profiles measured by analysis of Electron Cyclotron Emission [43] and far infrared interferometry [44] respectively, or by Thomson scattering of a ruby laser [45] for both quantities. Differences were found between the radial profiles measured by the above methods (typically 15% $T_e(r)$ and 25% in $N_e(r)$ for a given radius) with consequent variations in the calculated position of the Cl XVI emission shell. However the values of T_e and N_e at this calculated radial position were typically within 10% provided that the same measurements of T_e and N_e which were input to the transport code were used in the matching of the calculated emission shell position with the T_e and N_e profiles.

Fig.2 shows an example of the He-like spectra obtained. In addition to the four principal lines, three n = 2 satellites to the resonance line, q: $1s^22s\ ^2S_{1/2}$ - $1s(2s2p\ ^1P)\ ^2P_{3/2}$, r: $1s^22s\ ^2S_{1/2}$ - $1s(2s2p\ ^1P)\ ^2P_{1/2}$, and k: $1s^22p\ ^2P_{1/2}$ - $1s2p^2\ ^2D_{3/2}$ (labelled according to Gabriel [46]), are seen as well as some features on the long wavelength side of the resonance line indicating higher $n(\geq 3)$ satellites such as the d_{13} line [46].

The measurements were taken during the ohmic heating phase of the JET pulse. The experimental results were reproducible from pulse to pulse and for illustrative purposes in this paper data are cited from five separate pulses. The spatial Cl XVI emission profiles provided by the transport code showed that the emission occurred from a localised shell approximately 45-55cm from the centre of the plasma, in which N_e and T_e did not vary by more than 25%, log T_e being within 35% of the temperature of maximum emissivity of the resonance line in coronal equilibrium. This was calculated to be log $T_m = 7.2$, where T_e is measured in K, and is in agreement with the result of Gabriel [46].

The contribution of unresolved satellites was estimated using the data of Vainshtein and Safronova [47] and Bhalla et al [48] . The forbidden line at 4.4970Å could not be resolved from the satellite line j; $1s^2 2p\ ^2P_{3/2}$ - $1s2p^2\ ^2D_{5/2}$, and its enhancement of the forbidden line intensity was estimated to be $\simeq 11\%$. There was no significant change in the sensitivity of the spectrometer over the wavelength range under investigation and hence no corrections were made for this in the calculations.

4. Results and Discussion

Using the statistical balance population code of Summers et al [34] in conjunction with the atomic data discussed in section 2, coronal Cl XVI excited state populations were calculated for a range of electron temperatures and densities. Photoexcitation and de-excitation processes are negligible in comparison with the corresponding collisional processes and all transitions were considered optically thin. Hence theoretical R and G ratios were derived.

The temperature sensitive G ratio is plotted in fig.3 both with and without recombination included. In the density range log $N_e = 12.0$ to log $N_e = 14.0$, for which theoretical ratios were calculated, G showed no sensitivity to density. At higher densities G will become density sensitive due to increased population of the $1s2p\ ^1P$ state by collisional excitation of the $1s2s\ ^1S$ level [49] . Fig.3 also shows the comparison between theoretical and observed values of G. The measured values of T_e at the position of the Cl XVI shell ranged in JET from approximately log $T_e = 7.29$ to log $T_e = 7.44$, with a density range of log $N_e = 13.3$ to log $N_e = 13.5$. In this temperature range the theoretical curve is approaching a minimum before increasing again, due to increased recombinations into the triplet states as the temperature increases [35]. The average difference between the experimental and theoretical results in this region is typically 10% which is within experimental uncertainties.

The model calculations assume coronal equilibrium which is valid in the centre of tokamak plasmas [39] [50], whereas the Cl XVI emission shell in JET is typically located some distance from the minor axis. In fig.3 the effect of substituting for the coronal balance a diffusive ionisation model calculated from the transport code [42] is also shown. This model is dependent on the input radial profiles of electron temperature and density, and takes account of radial impurity transport using the radial profiles for the diffusion coefficient and inward convective velocity derived by Pasini et al [51]. At temperatures between log $T_e = 7.2$ and $T_e = 7.4$ the re-evaluated G ratio is much the same as the original calculation, however below this temperature range the new value of the ratio rises above the coronal case. This calculation could only be made for temperatures up to log

$T_e = 7.4$ as this was the maximum temperature attained during the ohmic phase of the discharges studied. Fig.4 plots ionisation fractions for Li, He and H like chlorine as a function of major radius for both the coronal case and that calculated for JET, where the temperatures log $T_e = 7.4$and $T_e = 7.2$ correspond to a radii of about 3.5 and 3.78m respectively. Between these radii the coronal and JET ionisation balances are similar and hence so are the calculated ratios (see fig.3). At greater radii there is a departure from the coronal case with an increased H-like to He-like ratio. For example at log $T_e = 7.15$ (R = 3.83m) this ratio is 43% larger for JET than for the coronal case. This results in increased recombinations into the triplet states and the corresponding rise in the G ratio as shown. In general the effect of diffusion on the equilibrium condition is to push the peaks of the emisson shells towards smaller radii than is the case for with a coronal balance.

In fig.5 the theoretical R ratio is plotted as a function of electron density for electron temperatures ranging from log $T_e = 6.4$ to log $T_e = 7.6$. It exhibits no significant density dependence below log $N_e = 13.5$ being in its low density limit, R_o, where there is no collisional coupling between the metastable $1s2s\ ^3S$ state and the $1s2p\ ^3P$ states [35] . Hence over the range of the JET experimental results the ratio R is unusable as a density diagnostic but can function as a measure of electron temperature to a limited extent, varying by a factor of approximately 1.5 over the temperature range shown. Exclusion of radiative and dielectronic recombination of H-like Cl causes the value of R_o to decrease, an effect which is enhanced with increasing temperature. This results in a decrease in temperature sensitivity for densities below R_o. For example at log $N_e = 13$ R changes by a factor of about 1.5 over the temperature range log $T_e = 6.4$ to log $T_e = 7.6$ if recombination effects are included compared to a variation of 1.1 if they are excluded from the calculations.

Fig.5 also shows the observed values of R from JET, which agree to within 7% of the theory, and a theoretical point resulting from substitution of an ionisation balance calculated for JET conditions at an electron temperature of log $T_e = 7.41$ and an electron density of log $N_e = 13.4$, as for the G ratio. Again this point is similar to the coronal calculation for the same density and temperature. Calculations for lower temperatures show only a small departure from the coronal case, as recombination occurs into both upper and lower levels of the ratio and hence has little effect.

Similar work for Cl XVI has been carried out by Källne et al [23] on the Alcator-C tokamak where measurements have been made at higher densities with the R ratio no longer in its low density limit, and also over a greater temperature range than the results measured here (the JET measurements are viable as a means of verifying R_o and the value of G over a limited temperature range, but do not occur in regions which are particularly sensitive with respect to electron density and temperature diagnostics). In addition coronal equilibrium calculations have been undertaken by Källne for both ratios with ionization and recombination effects included. Inward diffusive effects were not included in these calculations. The Källne experimental ratios are taken from a single discharge in this paper (see figs.6 and 7), but two discharges were discussed by Källne. The ratios from these two discharges were non-reproducible. The results for the discharge shown in this paper are preferred as they are in better agreement with the Källne theory for the G ratio (both sets

of Källne experimental R ratios agreed equally with their theoretical R ratio) and are consistent with values from the JET pulses shown, as well as with the present theoretical calculations.

Fig.6 shows the difference between the Källne and current calculations for the variation of the R ratio with electron density at $T = T_m$ for a coronal ionisation balance. There is a significant difference for the value of R_o at $T = T_m$, the present result being approximately 23% smaller than that of Källne et al. This decrease is consistent with results obtained for Al XII, Si XIII and S XV using the same method of calculation [52]. The JET experimental results for R_o, which lie above T_m, are included as they are still below the Källne value for R_o. The discrepancy between the two theoretical curves decreases with density above R_o to an intersection at log $N_e \simeq 14.3$, after which it increases. For example the value of R for this paper is almost a factor of three greater than the Källne value at log $N_e = 15.5$. The Källne experimental points lie in the region log $N_e = 14$ to log $N_e = 15$ which is above the low density limit where the JET measurements occur, and the present theory typically agrees to within 20% of the Källne experimental data at these higher densities. Contributions from dielectronic satellites to the experimental data are considered by Källne as for the the JET results, with a reduction the intensity of the forbidden line of approximately 15%.

The comparison between the Källne results and those of this paper for the G ratio is given in fig.7. The Källne calculations cover a smaller temperature range but the slope should decrease at higher temperatures ($T > T_m$) as for the current results. The average difference between the two sets of calculations for the temperature range shown is approximately 20%. Experimental points from the Källne paper measured over a wider range in temperatures than the JET results are also included . These do not consider satellite contributions to the forbidden line, a factor which would tend to reduce the experimental values improving agreement with theory from this paper.

5.Conclusion

Improved electron impact excitation rates have been used to derive R and G ratios for He-like Cl which show significant differences from those of previous authors. R_o and G vary by factors of approximately 1.5 and 1.9 respectively over the temperature range log $T_e = 6.4$ to log $T_e = 7.6$, which is comparable with similar calculations for other helium-like ions [39,52] . The theoretical R ratio shows strong density dependence above its low density limit, varying by about a factor of about 10 over the density range log $N_e = 13.5$ to log $N_e = 16$ at log $T_e = 7.6$.

Comparison of the theoretical calculations with the JET experimental results (figs. 3 to 7) reveals typical discrepancies in R and G of 7% and 10% respectively. However JET data covers a narrow temperature range and is in the low density limit. The experimental results of Källne et al which have a wider temperature range and are in the density sensitive region, are also in agreement with the current theory, giving a good indication of the accuracy of the atomic data used in the line ratio calculations. Re-evaluation of the theoretical ratios using an ionisation balance calculated for conditions in JET, produced a departure from the coronal based calculations for the G ratio. This does not produce significant differences at the radial position of the Cl XVI emission shell, but will affect measurements taken at greater radii where the temperature is lower.

Although such ratios are not routinely used as electron temperature and density diagnostics on devices such as JET, non-spectroscopic techniques being preferred [42-44], they may be applied to the analysis of such sources for which no independent estimates of these parameters exist (such as the solar corona).

Acknowledgement

We would like to thank Professor A.E.Kingston, Dr. P.R.Thomas and Dr. R.Giannella for their interest in the work, to L.Lauro-Taroni for use of the SANCO code, and to Professor H.P.Summers for use of the ADAS codes. IHC is grateful to the Culham Laboratory for financial support. The authors are indebted to the staff involved at the JET and Culham laboratories. WJD is on long term secondment from the Department of Physics and Applied Physics, University of Strathclyde. This work was supported by the Nuffield Foundation.

References

1. Lee, P., Leiber, A.J., Pradhan, A.K. and Xu, Y., Phys. Rev. A34, 3210 (1986)

2. Kolk, K.H., Konig, R. and Kunze, H.J., Phys. Rev. A33, 747 (1986)

3. McKenzie, D.L., Landecker, P.B., Feldman, U. and Doschek, G.A., Astrophys. J. 289, 849 (1985)

4. Phillips, K.J.H. *et al*, Astrophys. J. 256, 774 (1982)

5. Acton, L.W., Bruner, M.E., Brown, W.A., Fawcett, B.C., Schweizer, W. and Speer, R.J., Astrophys. J. 291, 865 (1985)

6. Gabriel, A.H. and Jordan, C., Mon. Not. R. Astron. Soc. 145, 241 (1969)

7. Blumenthal, G.T., Drake, G.W.F. and Tucker, W.H., Astrophys. J. 172, 205 (1972)

8. Mohr, P.J., Beamfoil Spectroscopy, Plenum Press: New York Vol.2, (1975)

9. Henry, R.J.W., Phys. Rep. 68, 1 (1981)

10. Pradhan, A.K., Astrophys. J. Suppl. 59, 183 (1985)

11. Eissner, W. and Seaton, M.J., J. Phys. B5, 2178 (1972)

12. Burke, P.G. and Robb, W.D., Adv. At. Mol. Phys. 11, 143 (1975)

13. Tayal, S.S. and Kingston, A.E., J. Phys. B17, L145 (1984)

14. Tayal, S.S. and Kingston, A.E., J. Phys. B17, 1383 (1984)

15. Tayal, S.S. and Kingston, A.E., J. Phys. B18, 2983 (1985)

16. Kingston, A.E. and Tayal, S.S., J. Phys. B16, L53 (1983)

17. Kingston, A.E. and Tayal, S.S., J. Phys. B16, 3465 (1983)

18. Tayal, S.S., Phys. Rev. A34, 1847 (1986)

19. Tayal, S.S., Phys. Rev. A35, 2073 (1987)

20. Keenan, F.P., McCann, S.M. and Kingston, A.E., Physica Scripta, 35, 432 (1987)

21. Gabriel, A.H. and Jordan, C., Case Studies in Atomic Collision Physics, Amsterdam:North Holland, 2, 209 (1972)

22. Wolfson, C.J., Doyle, J.G., Leibacher, W.J. and Phillips, K.J.H, Astrophys. J. 269, 319 (1983)

23. Källne, E., Källne, J. and Pradhan, A.K., Phys. Rev. A27, 1476 (1983)

24. Kelly, R.L., Oakridge National Lab., ORNL-5922, (1982)

25. Zang, H. and Sampson, D.H., Ap. J. Suppl. 63, 487 (1987)

26. Gabriel, A.H., and Heddle, D.W.O., Proc. Roy. Soc. London, A258, 124 (1960)

27. Lin, D.C., Johnston, W.R. and Dalgarno, A., Phys. Rev. A15, 154 (1977)

28. Laughlin, C., J. Phys. B11, L391 (1978)

29. Kahn, F. and Khandelwal, G.S., Astrophys. J. 329, 493 (1988)

30. Cohen, M. and McEachran, R.P., Canadian Journal of Physics, 50, 1363 (1972)

31. Jacobs, V.L., J.Phys. B5, 213 (1972)

32. Lin, D.C., Johnston, W.R. and Dalgarno, A., Astrophys. J. 217, 1011 (1977)

33. Mewe, R. and Schriver, J., Astron. Astrophys. 65, 99 (1978)

34. Summers, H.P., Briden, P., Dickson, W.J. and Lang, J., "An Atomic Data & Analysis Structure for Spectral Emission in Laboratory and Astrophysical Plasmas" - to be published.

35. Pradhan, A.K. and Shull, J.M., Astrophys. J. 249, 821 (1981)

36. Seaton, M.J., Mon. Not. R. Astron. Soc. 127, 191 (1964)

37. Keenan, F.P. and Reid, R.G.H, J.Phys. B20, L753 (1987)

38. Keenan, F.P. and Reid, R.H.G., Physica Scripta 39, 314 (1989)

39. Keenan, F.P., McCann, S.M., Barnsley, R., Dunn, J., Evans, K.D. and Peacock, N.J., Phys. Rev. A39, 4092 (1989)

40. Rebut, P.H. *et al*, Fus. Tech. 11, Vol.1 (1987)

41. Barnsley, R., Schumacher, U., Källne, E., Morsi, H.W. and Rupprecht, G., Rev. Sci. Inst. (1991) (in press)

42. Lauro-Taroni, L., JET Laboratory, private communication.

43. Costley, A., Diagnostics for Fusion Reactor Conditions, EUR 83 51-1 EN. Comission of the European Communities Brussels, 129 (1982)

44. Orlinski, D.V. and Magyar, G., Nucl. Fusion, 29, 611 (1988)

45. Salzmann, H., Hirsch, K., Rohr, J., Bredlow, G. and Witte, K., Rev. Sci. Inst. 56, 1030 (1985)

46. Gabriel, A.H., Mon. Not. R. Astr. Soc. 160, 99 (1972)

47. Vainshtein, L.A. and Safronova, U.I, At. Data. Nucl. Data. Tables, 21, 49 (1978)

48. Bhalla, C.P., Gabriel, A.H. and Presnyakov, L.P., Mon. Not. R. Astr. Soc. 172, 359 (1975)

49. McKenzie, D.L., Astrophys. J. 249, 821 (1981)

50. Hinnov, E., "Diagnostics for Fusion Experiments", Proceedings of the International School of Plasma Physics, Varenna, Italy, (E.Sindoni and C.Wharton, eds.), Pergammon, Oxford, 139 (1980)

51. Pasini, D., Mattioli, M., Edwards, A.W., Giannella, R., Gill, R.D., Hawkes, N., Magyar, G., Saoutic, B., Wang, Z. and Zasche, D., Nucl. Fusion 30, 2049 (1990)

52. McCann, S.M. and Keenan, F.P., J. Phys. Colloque. 49, C1-331 (1988)

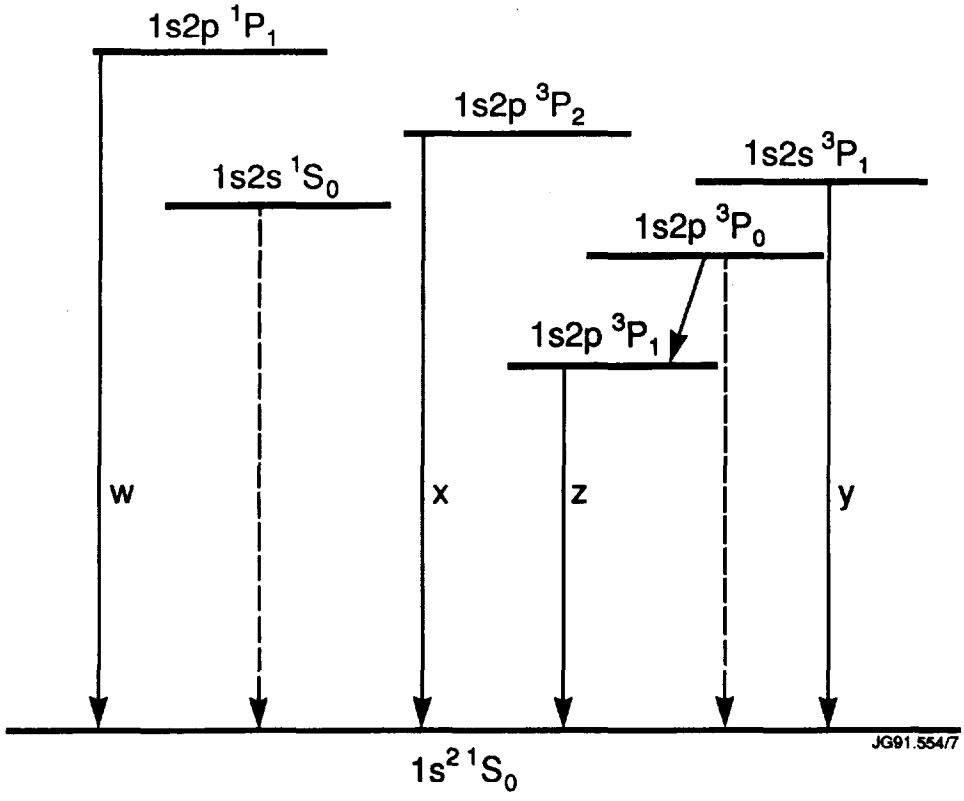

Fig.1 Energy level diagram for the ground state and first excited configuration in a He-like atom.

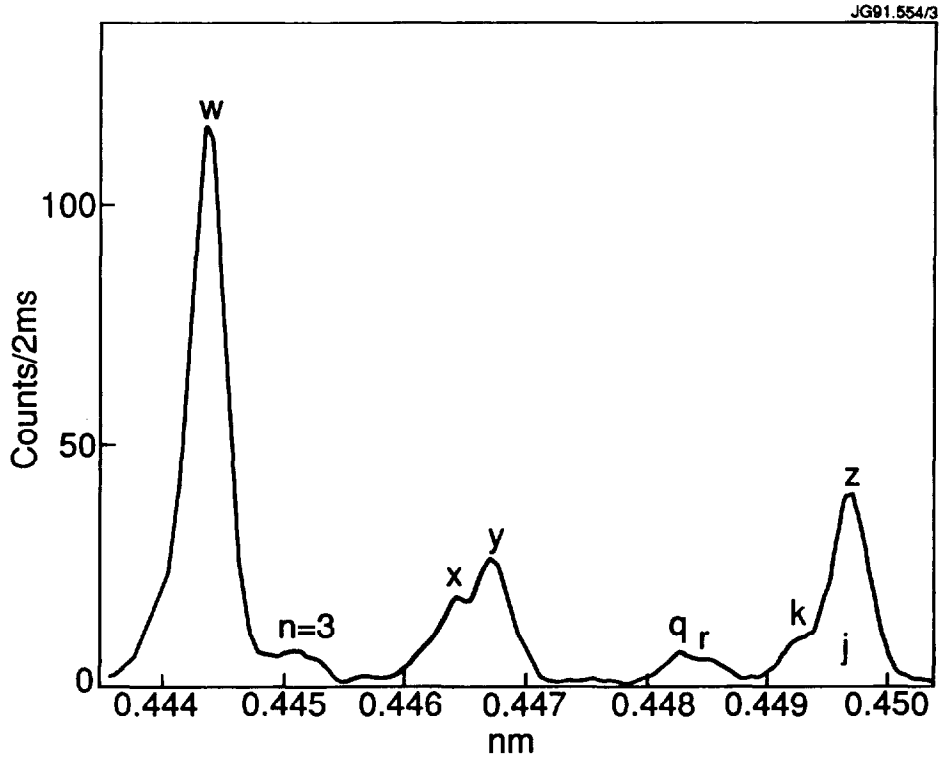

Fig.2 Measured spectrum from JET for He-like chlorine. As well as the resonance line w, the intercombination lines x and y and the forbidden line z, four dielectronic satellite lines, d_{13}, q, r and k are shown. Also labelled is the j line which is not resolved from the forbidden line in this study.

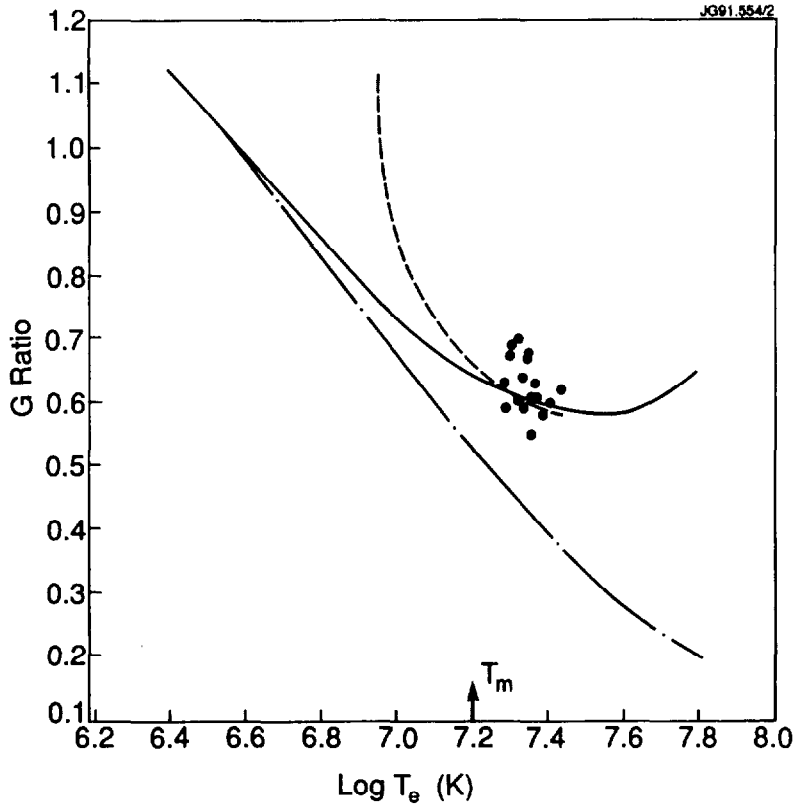

Fig.3 The theoretical emission ratio G plotted as a function of electron temperature T_e (in units of degrees Kelvin) at an electron density of log $N_e = 13.5$, with dielectronic and radiative recombination included in (solid line) or excluded from (broken line) the calculations. Typical errors in the JET experimental data (solid points) which are measured at densities ranging from log $N_e = 13.2$ to log $N_e = 13.4$, are $\pm$ 12% in G_{obs} and $\pm$ 0.09 in log T_e. Also included (dashed line) is the theoretical G ratio calculated using an ionisation balance calculated for typical JET plasma conditions.

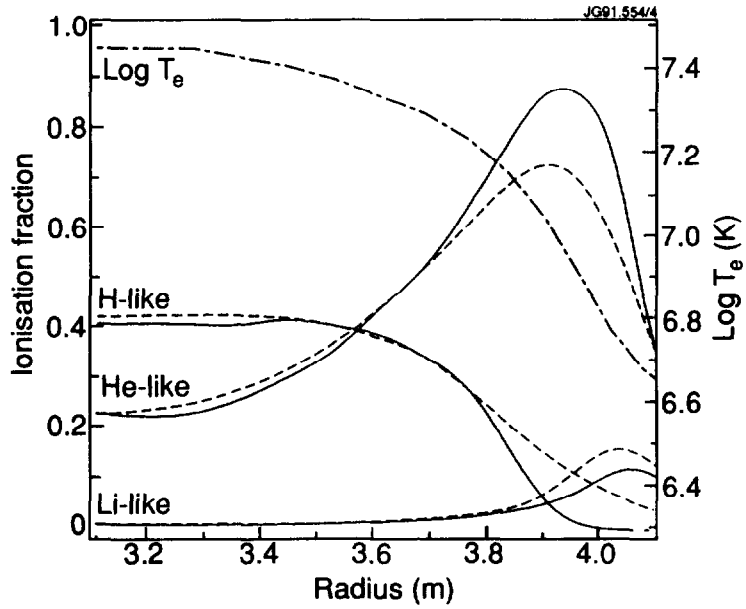

Fig.4 Ionisation fractions of H-like, He-like and Li-like Cl as a function of radius for a typical JET pulse (dashed lines), and the coronal equivalent for the same temperature and density conditions (solid lines). The relevant electron temperature profile (broken line, in units of degrees Kelvin) is also shown.

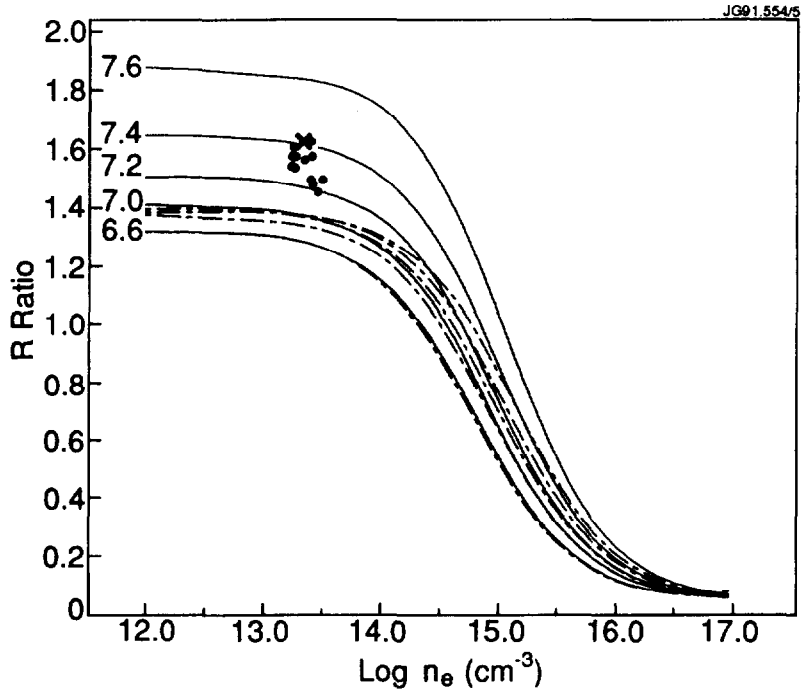

Fig.5 The theoretical emission line ratio R plotted as a function of electron density, with the present calculations plotted at electron temperatures (top to bottom), log T_e = 7.6, 7.4, 7.2, 7.0, and 6.4, with dielectronic and radiative recombination included (solid lines) or excluded (broken lines). Also shown (cross) is the theoretical R ratio calculated using a non coronal ionisation balance at an electron temperature of log T_e = 7.41 and an electron density of log N_e = 13.4. Typical errors in the JET experimental data (dots, measured at electron temperatures ranging from log T_e = 7.29 to log T_e = 7.44) are ± 8.0% in R_{obs} and ± 0.06 in log N_e.

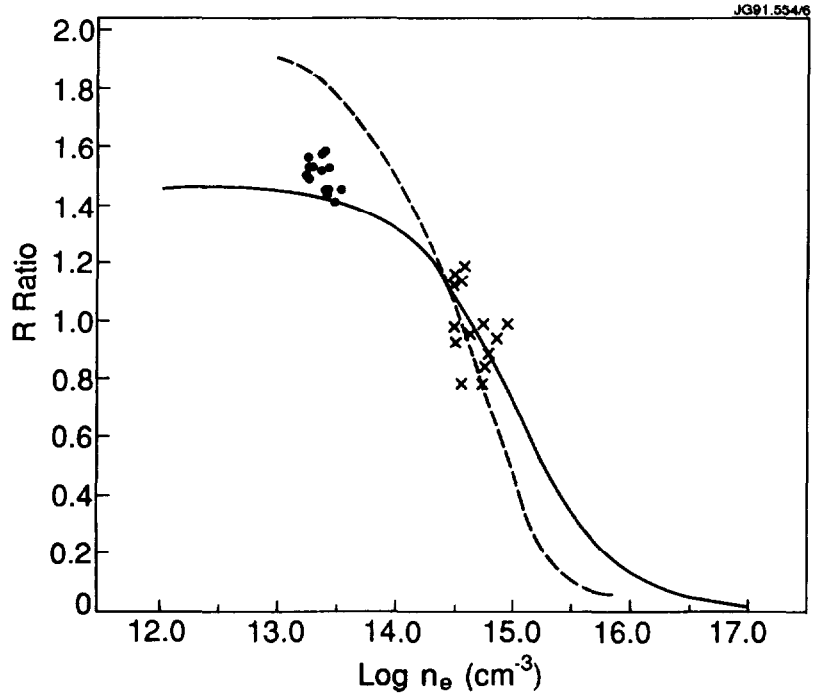

Fig.6 The theoretical emission line ratio R plotted as a function of electron density, with the present calculations (solid line, with dielectronic and radiative recombination) and the calculations of Källne et al [22] (dashed line) both plotted for log T_e = 7.2. The experimental data from JET (solid points, at temperatures ranging from log T_e = 7.29 to log T_e = 7.44) and Källne et al (crosses, at a temperature of log T_e = 7.2) are also shown.

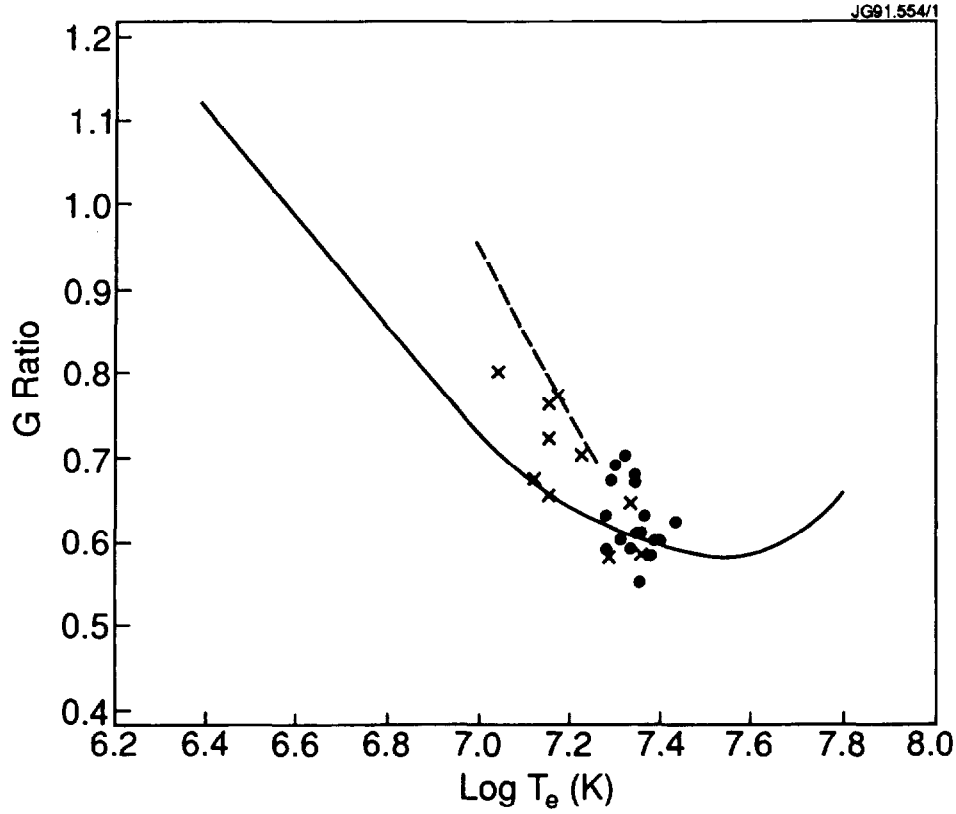

Fig.7 The theoretical emission ratio G plotted as a function of electron temperature T_e (in units of degrees Kelvin, with the present calculations (solid line, with dielectronic and radiative recombination) and the calculations of Källne et al [22] (dashed line). Experimental values are also shown with current measurements from JET (solid points) and those of Källne et al (crosses).

Appendix I

THE JET TEAM

JET Joint Undertaking, Abingdon, Oxon, OX14 3EA, U.K.

J.M. Adams[1], H. Altmann, A. Andersen[14], P. Andrew[18], M. Angelone[29], S.A. Arshad, W. Bailey, P. Ballantyne, B. Balet, P. Barabaschi, R. Barnsley[2], M. Baronian, D.V. Bartlett, A.C. Bell, I. Benfatto[5], G. Benali, H. Bergsaker[11], P. Bertoldi, E. Bertolini, V. Bhatnagar, A.J. Bickley, H. Bindslev[14], T. Bonicelli, S.J. Booth, G. Bosia, M. Botman, D. Boucher, P. Boucquey, P. Breger, H. Brelen, H. Brinkschulte, T. Brown, M. Brusati, T. Budd, M. Bures, T. Businaro, P. Butcher, H. Buttgereit, C. Caldwell-Nichols, D.J. Campbell, P. Card, G. Celentano, C.D. Challis, A.V.Chankin[23], D. Chiron, J. Christiansen, C. Christodoulopoulos, P. Chuilon, R. Claesen, S. Clement, E. Clipsham, J.P. Coad, M. Comiskey[4], S. Conroy, M. Cooke, S. Cooper, J.G. Cordey, W. Core, G. Corrigan, S. Corti, A.E. Costley, G. Cottrell, M. Cox[7], P. Cripwell, H. de Blank[15], H. de Esch, L. de Kock, E. Deksnis, G.B. Denne-Hinnov, G. Deschamps, K.J. Dietz, S.L. Dmitrenko, J. Dobbing, N. Dolgetta, S.E. Dorling, P.G. Doyle, D.F. Düchs, H. Duquenoy, A. Edwards, J. Ehrenberg, A. Ekedahl, T. Elevant[11], S.K. Erents[7], L.G. Eriksson, H. Fajemirokun[12], H. Falter, D. Flory, J. Freiling[15], C. Froger, P. Froissard, K. Fullard, M. Gadeberg, A. Galetsas, D. Gambier, M. Garribba, P. Gaze, R. Giannella, A. Gibson, R.D. Gill, A. Girard, A. Gondhalekar, C. Gormezano, N.A. Gottardi, C. Gowers, B.J. Green, R. Haange, G Haas, A. Haigh, G. Hammett[6], C.J. Hancock, P.J. Harbour, N.C. Hawkes[7], P. Haynes[7], J.L. Hemmerich, T. Hender[7], F.B. Herzog, R.F. Herzog, J. Hoekzema, J. How, M. Huart, L Hughes, T.P. Hughes[4], M. Hugon, M. Huguet, A. Hwang[7], B. Ingram, M. Irving, J. Jacquinot, H. Jaeckel, J.F. Jaeger, G. Janeschitz[13], S. Jankowicz[22], O.N. Jarvis, F. Jensen, E.M. Jones, L.P.D.F. Jones, T.T.C. Jones, J-F. Junger, E. Junique, A. Kaye, B.E. Keen, M. Keilhacker, G.J. Kelly, W. Kerner, R. Konig, A. Konstantellos, M. Kovanen[20], G. Kramer[15], P. Kupschus, R. Lässer, J.R. Last, B. Laundy, L. Lauro-Taroni, K. Lawson[7], M. Lennholm, A. Loarte, R. Lobel, P. Lomas, M. Loughlin, C. Lowry, B. Macklin, G. Maddison[7], G. Magyar, W. Mandl[13], V. Marchese, F. Marcus, J. Mart, E. Martin, R. Martin-Solis[8], P. Massmann, G. McCracken[7], P. Meriguet, P. Miele, S.F. Mills, P. Millward, R. Mohanti[17], P.L. Mondino, A. Montvai[3], S. Moriyama[28], P. Morgan, H. Morsi, G. Murphy, M. Mynarends, R. Myrnäs[16], C. Nardone, F. Nave[21], G. Newbert, M. Newman, P. Nielsen, P. Noll, W. Obert, D. O'Brien, J. O'Rourke, R. Ostrom, M. Ottaviani, M. Pain, F. Paoletti, S. Papastergiou, D. Pasini, A. Peacock, N. Peacock[7], D. Pearson[12], R. Pepe de Silva, G. Perinic, C. Perry, M. Pick, R. Pitts[7], J. Plancoulaine, J-P. Poffé, F. Porcelli, L. Porte[19], R. Prentice, S. Puppin, S. Putvinsko[23], G. Radford[9], T. Raimondi, M.C. Ramos de Andrade, P-H. Rebut, R. Reichle, E. Righi, F. Rimini, D. Robinson[7], A. Rolfe, R.T. Ross, L. Rossi, R. Russ, P. Rutter, H.C. Sack, G. Sadler, G. Saibene, J.L. Salanave, G. Sanazzaro, A. Santagiustina, R. Sartori, C. Sborchia, P. Schild, M. Schmid, G. Schmidt[6], B. Schunke, S.M. Scott, A. Sibley, R. Simonini, A.C.C. Sips, P. Smeulders, R. Stankiewicz[27], M. Stamp, P. Stangeby[18], D.F. Start, C.A. Steed, D. Stork, P.E. Stott, T.E. Stringer, P. Stubberfield, D. Summers, H. Summers[19], L. Svensson, J.A. Tagle[21], A. Tanga, A. Taroni, A. Tesini, P.R. Thomas, E. Thompson, K. Thomsen, J.M. Todd, P. Trevalion, B. Tubbing, F. Tibone, E. Usselmann, H. van der Beken, G. Vlases, M. von Hellermann, T. Wade, C. Walker, R. Walton[6], D. Ward, M.L. Watkins, M.J. Watson, S. Weber[10], J. Wesson, T.J. Wijnands, J. Wilks, D. Wilson, T. Winkel, R. Wolf, B. Wolle[24], D. Wong, C. Woodward, Y. Wu[25], M. Wykes, I.D. Young, L. Zannelli, Y. Zhu[26], W. Zwingmann.

PERMANENT ADDRESSES

1. UKAEA, Harwell, Didcot, Oxon, UK.
2. University of Leicester, Leicester, UK.
3. Central Research Institute for Physics, Academy of Sciences, Budapest, Hungary.
4. University of Essex, Colchester, UK.
5. ENEA-CNR, Padova, Italy.
6. Princeton Plasma Physics Laboratory, New Jersey, USA.
7. UKAEA Culham Laboratory, Abingdon, Oxon, UK.
8. Universidad Complutense de Madrid, Spain.
9. Institute of Mathematics, University of Oxford, UK.
10. Freien Universität, Berlin, F.R.G.
11. Swedish Energy Research Commission, S-10072 Stockholm, Sweden.
12. Imperial College of Science and Technology, University of London, UK.
13. Max Planck Institut für Plasmaphysik, Garching bei München, FRG.
14. Risø National Laboratory, Denmark.
15. FOM Instituut voor Plasmafysica, 3430 Be Nieuwegein, The Netherlands.
16. University of Lund, Sweden.
17. North Carolina State University, Raleigh, NC, USA
18. Institute for Aerospace Studies, University of Toronto, Downsview, Ontario, Canada.
19. University of Strathclyde, 107 Rottenrow, Glasgow, UK.
20. Nuclear Engineering Laboratory, Lapeenranta University, Finland.
21. CIEMAT, Madrid, Spain.
22. Institute for Nuclear Studies, Otwock-Swierk, Poland.
23. Kurchatov Institute of Atomic Energy, Moscow, USSR
24. University of Heidelberg, Heidelberg, FRG.
25. Institute for Mechanics, Academia Sinica, Beijing, P.R. China.
26. Southwestern University of Physics, Leshan, P.R. China.
27. RCC Cyfronet, Otwock Swierk, Poland.
28. JAERI, Naka Fusion Research Establishment, Ibaraki, Japan.
29. ENEA, Frascati, Italy.

At 1st June 1991